SimBuild 2006

Second National IBPSA-USA Conference
Cambridge, MA
August 2-4, 2006

USING SIMULATION TOOLS IN A UNIVERSITY LABORATORY COURSE: ASSESSING THE PERFORMANCE OF A HEALTH-CARE CENTER IN LUSAKA, ZAMBIA

Leslie K. Norford
Building Technology Program
Department of Architecture
Massachusetts Institute of Technology
Cambridge, MA 02139

ABSTRACT

As part of a building-technology laboratory class, students were asked to evaluate the performance of a proposed health-care center for Lusaka, Zambia. The building was designed to be constructed at modest cost, operated at very low cost and as independently as possible of utility services, and comfortable throughout the year with no active heating or cooling. The evaluation consisted of a combination of scale-model measurements and simulation. Daylighting was simulated with a simple CAD model and a radiosity-based program, with attention to surface properties. Wind-driven airflows were measured in a 1:24 scale model of the cluster of buildings that comprise the health-care center, converted to air-change rates, and scaled to the full-size buildings. Buoyancy-driven flows were simulated in a nodal-analysis program. Airflow rates were imported into a one-node dynamic thermal-analysis program to estimate diurnal temperatures and evaluate thermal comfort. Retention of rainwater for use in toilets, evaporative cooling of ventilation air, and generation of electricity from photovoltaic panels were also calculated. Results indicated that interior spaces were generally well lit during daylight hours and that peak indoor temperatures were no higher than the outdoor peak values, which vary from 21 to 30 ^{o}C seasonally.

INTRODUCTION

Most students in the undergraduate, pre-professional architecture program at MIT take a technology laboratory class that focuses on passive strategies for conditioning buildings and emphasizes applications in developing countries. While the lab projects have varied from year to year, many have required a comparison of measurements and simulations. This comparison is effective only if the simulation tools can be learned in a relatively short period of time and if the simulation inputs can be readily adjusted to match experimental conditions. Further, the lectures in the course stress fundamental mass and energy balances and simulation tools have been developed or selected to show how fundamental equations can be automated; in short, the transparency of the simulation program is important.

In the most recent course, students designed, constructed and tested small (0.03-0.06 m^3) passive-solar, single-zone "elf houses," using a simple single-node (one thermal resistor and one thermal capacitor) dynamic model as a design tool to assess the impact of variations in wall construction and in the size, orientation and construction of windows. Predictions of indoor temperatures, made with measurements and estimates of actual temperature and solar radiation, were then compared with measurements made with small, temperature data loggers. The single-node model followed directly from a dynamic energy balance but could not distinguish the temperatures of the indoor air, dedicated thermal-mass introduced to absorb direct solar radiation, and the walls, nor could it differentiate the placement of insulation inside or outside wall mass. To account for these effects, the single-node model was extended to a system of coupled first-order equations, solved in a standard mathematical programming package (Mathworks 2006). The simulation programs were not as comprehensive as those that incorporate the heat-balance method but met the above-mentioned criteria and for many models offered results in reasonable agreement with data.

In another project, students modeled houses in villages in Gujarat, India and measured daylight levels under conditions that mimicked different dates and times in Gujarat. Students then designed openings to improve the indoor lighting to levels they considered adequate for hypothesized tasks, using the daylight-factor method or the lumen-method for skylights and windows; modified the models; and took another round of measurements. They compared the measurements with their targets and with estimates made with a CAD model imported into a radiosity-based lighting-simulation program (Lightscape 1999). Careful attention was paid to surface reflectances, via measurements of materials in

use in Gujarati houses, application of paints and other materials to models to achieve the target reflectances, and adjustment of reflectances in the simulation program. Use of this program was facilitated by an excellent tutorial, a series of example files and accompanying text that students could work through on their own in a modest amount of time.

In lieu of a laboratory project focused on airflow, as was done in several past years, the last of three projects was shifted to consider a health-care center in Lusaka, Zambia. This center was designed by an architecture professor at MIT for a non-profit organization that intends to build a series of such centers for AIDS patients in Africa. Passive cooling and lighting strategies were considered to be essential to provide thermally and visually comfortable buildings at minimum cost. Students in the laboratory class were no longer using simulation and measurement to assess and improve their own designs but instead were asked to provide technical feedback to the designer before construction. Teams of 2-4 students were asked to consider individual buildings in the clinic and evaluate them in terms of daylight, airflow and indoor temperatures. Additional work was done to assess storage of rainwater for use on site during dry months and to size photovoltaic panels for electricity. This paper describes the buildings and site, and summarizes model-based measurements and simulations in each of the above areas.

Professional consultants asked to evaluate this project would likely use a different set of tools. However, the time constraints of the laboratory course and its constituency, primarily students of architectural design, made the assignment somewhat similar to what designers with some technical understanding might do in practice: judge a design as quickly and accurately as possible, before locking into one solution.

BUILDING AND SITE DESIGN

The proposed health-care center consists of several buildings on a 0.2 ha site in Lusaka, Zambia. The buildings were designed for a non-profit organization that intends to build a series of such centers in Africa. Figure 1 presents a view of the site and buildings from the east. The building in the foreground is a service center that includes a two-person patient room and a laundry, kitchen and staff lounge plus a storage shed. Behind it, at a slight angle, is a patient ward that consists of four rooms, each with four beds. To the right, or south, of the patient ward is an education building that will house a pharmacy, examination room, office, and children's daycare and play facility. At the southeast corner of the site is an insaka, a traditional outdoor public meeting place, and along the northern boundary is a small chapel with a concave roof. The buildings will be constructed of concrete block coated with plaster; roofs are corrugated metal and thatch.

As shown in Figure 2 (with data taken primarily from Washington Post 2006), the climate in Lusaka is warm and somewhat humid. Monthly average maximum temperatures range from 21 ^{o}C in winter to nearly 30 ^{o}C in summer. The maximum monthly average temperature (estimated as the mean of maximum and minimum) is 25 ^{o}C, in October. Applying the adaptive-thermal comfort standard in ASHRAE Standard 55-2004 (ASHRAE 2004), the maximum operative temperature at the 80% acceptability limit is about 29 ^{o}C, 1 ^{o}C lower than the average daytime peak temperature. The diurnal temperature variation is small in summer, about 5 ^{o}C, and larger in winter, 10-12 ^{o}C.

Rainfall is highly seasonal (BBC 2006). The average yearly total is 0.84 m, almost all of which falls in the warmer half of the year, November-April.

Figure 1. A model of the proposed health-care center in Lusaka, Zambia. North is to the right.

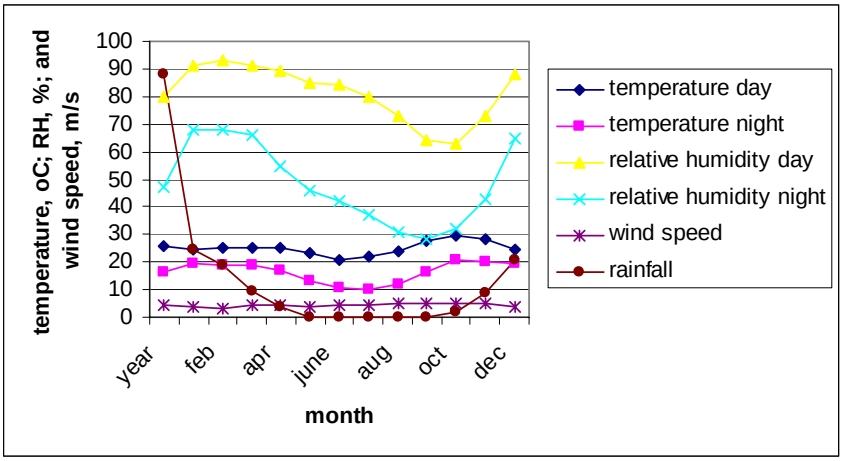

Figure 2. Climate data for Lusaka.

DAYLIGHTING

Lighting simulations for a room in the patient ward were performed for 9 a.m., noon and 3 p.m. for June 21 (winter solstice) and December 21 (summer solstice). A three-dimensional CAD model was imported into a radiosity-based lighting simulation program (Lightscape 1999) for the simulation. Based on prior investigations of surface reflectances, students selected values of 25%, 50% and 75% for the floor, walls and ceiling, respectively.

Results, shown in Figure 3, are presented as 50-5,000 lux (or lumen/m^2) logarithmic color scales; outdoor horizontal illuminance levels are shown for reference. June 21 was modeled as a clear day, based on the weather data shown in Figure 2. Illuminance levels in the patient room were generally 1,500-2,000 lx. The three recommended levels for common visual tasks are 300, 500 and 1,000 lx, with higher values appropriate for tasks of small size or low contrast (IES 2000); simulated levels provided ample light for reading. In the afternoon, however, direct sunlight strikes the area designated for patient beds. This could be controlled with window shades.

December 21 is in the rainy season and was modeled as being overcast. As shown by the colors in Figure 3, there is a larger spatial variation of indoor illumination,

500-2,500 lx. Beds closer to the western windows receive more light.

Occlusion of the sky and sun from neighboring buildings and trees was not modeled but would reduce the indoor illuminance levels, including the extreme, direct-sun conditions shown in Figure 3.

June 21

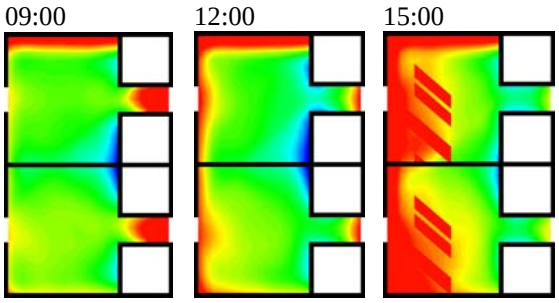

Figure 3. Illuminance levels in a patient room. East is to the right.

AIRFLOW

Airflows in the buildings were studied with experiments and simulation with a nodal model. Computational fluid dynamics (CFD) has been used for similar studies in other classes, with mixed success. When it has been taught in a way that meets the criteria defined above, it has worked well; this has required presentation of the conservation equations, discussion of their numerical solution, and We have a thorough, step-by-step tutorial that includes a number of examples with known results that students should be able to reproduce. Without a comprehensive tutorial, students typically made mistakes in setting up and running the simulations and were not able to discern the impact of their errors on the resulting flows. We found it necessary to prepare our own CFD tutorial, focused on wind- and buoyancy driven airflows in buildings. There was inadequate time in the study of the Zambia health-care center to learn to reliably use CFD.

Experiments were made with 1:24 scale models, constructed of thin sheets of rigid foam with a paper cover. Roofs were made of acetate to make indoor measurements possible and to see the movement of baby powder used to visualize the flow. Surfaces were painted black to enhance the contrast with the powder. The buildings were placed on a work table in locations that mimicked their position on the site, to account for wind shadows. Household fans were used to generate wind, at velocities on the order of 2 m/s. A hot-wire anemometer was used to take point measurements at interior locations and average readings over flow entrances and exits, including the clerestory windows. Figure 4 shows a model of the patient ward.

Figure 4. Airflow visualization and measurement model for the patient ward.

Flow visualizations showed the influence of the clerestory windows and neighboring structures. For example, air from the east flowed in the windows of the service building and out the west-facing clerestory. Air from the same direction flowed in the west-facing clerestory of the patient ward. The outdoor area in front of the service building was a recirculation zone when air came from the east, because the air had to flow over the service shed.

By computing average flow velocity over known opening areas and paying attention to flow direction, students were able to estimate air-change rates for their buildings. Air change rates in the model buildings were scaled to predict ventilation in the real buildings for wind speeds characteristic of Lusaka, using Equations 1 and 2.

$$ACH_m = \frac{WindowArea_m \cdot AirVelocity_m}{Volume_m} \cdot 3600 \qquad (1)$$

$$ACH_r = ACH_m \cdot \frac{AirVelocity_r}{AirVelocity_m} \cdot \frac{1}{n} \qquad (2)$$

where the subscripts m and r refer to the model and real buildings and n is the scale factor, in this case 24.

While the scaling is geometrically correct, it does not account for similitude requirements. To accurately predict full-scale flows with a model, the dimensionless form of the conservation-of-momentum equation shows that it is necessary to match the Reynolds number:

$$\mathrm{Re} = \frac{V_{ref} \cdot L_{ref}}{\nu} \qquad (3)$$

where V_{ref} and L_{ref} are reference velocities and lengths and n is the dynamic viscosity. In this case, air is used as the working fluid in the model and matching the Reynolds numbers yields the following requirement for air speed in the model tests:

$$V_{ref_m} = V_{ref_r} \cdot n \qquad (4)$$

Matching the Reynolds number for Lusaka air speeds of 5 m/s would have required a wind tunnel capable of producing 120 m/s. The window fan was limited to about 2 m/s. However, the Reynolds number for the model was 28,000, in the fully turbulent regime. Studies have shown that agreement between scale models and full-size buildings does not substantially degrade until the Reynolds number drops below 2,000 (as summarized in Walker 2006). Sample calculations are shown in Tables 1 and 2 for the education building and patient ward.

Table 1. Wind-driven airflow measurements and calculations for the education building.

	Model velocity, m/s for 2.5 m/s fan air speed	Model ACH	Calculated real ACH, for 3.9 m/s wind speed	Calculated real flow m^3/s
Wind from E	2.5			
playroom	0.50	1031	67	1.52
exam room	0.30	653	43	0.52
Wind from W	2.5			
playroom	1.40	3308	215	4.86
exam room	1.70	3703	240	2.95
Wind from S	2.5			
playroom	0.80	1654	60	1.35
exam room	0.45	980	36	0.43

Table 2. Wind-driven airflow measurements and calculations for the patient ward.

	Model velocity, m/s	Model ACH	Calculated real ACH	Calculated real flow, m^3/s
Room 1 door	0.27	401	17	0.54
Room 1 clerestory	0.59	1002	42	1.32
Room 2 door	0.39	580	24	0.76
Room 2 clerestory	0.65	1104	46	1.45
Room 3 door	1.46	2171	90	2.83
Room 3 clerestory	0.87	1478	62	1.95
Room 4 door	1.76	2617	109	3.43
Room 4 clerestory	0.96	1631	68	2.14

It would have been very difficult to use the models to estimate buoyancy-driven flows. The strict similarity requirement, matching the Grashof number, required impossibly large indoor temperatures in the model. The Grashof number is the square of the Reynolds number, with the air velocity due to buoyancy:

$$U_B = \sqrt{g\beta H\Delta T} \tag{5}$$

where g is the gravitational constant, β is the coefficient of thermal expansion, H is the height and ΔT is the indoor-outdoor temperature difference. Given the scaling factor of 24, the model temperature difference would need to be 24^3 times that in the real building.

Relaxing the matching condition in favor of achieving a critical value for the model Grashof number would have made the model tests more feasible (Walker 2006, Etheridge and Sandberg 1996); a Grashof number of nearly 10^6 could be achieved with a model ΔT of 1 K. Instead, we used a nodal airflow analysis program to estimate air-change rates due to buoyancy (CONTAM 2005). The program was not selected for wind-driven flows for two reasons: it does not provide flow patterns within a room and it requires user-provided estimates of the impact of wind shadows (i.e., air pressures at openings, rather than free-stream wind speeds), which in turn require experiments or CFD to determine.

The nodal-analysis program requires an a priori estimate of indoor temperature as input, but this temperature depends on the buoyancy flow for given heat gains. Students used a steady-state energy balance, Equation 6, with the volumetric airflow provided by the program, to check their initial estimate of indoor temperature; significant discrepancies were resolved by adjusting the temperature estimate and repeating the calculations.

$$q = \rho C_p V \Delta T \tag{6}$$

where q is the internal heat, ρ is the density, C_p is the specific heat, and V is the volumetric airflow.

Air-change rates for rooms in the patient ward were calculated to be 12-13 ACH when the doors were closed and 15-16 ACH when the doors were opened; these values corresponded to an indoor-outdoor temperature difference of 0.7-0.8 K.

INDOOR TEMPERATURE SIMULATION

It has been shown that thermal comfort requires that indoor temperatures during the warmest months be no higher and ideally slightly lower than outdoor temperatures. Internal heat gains tend to raise indoor temperatures but thermal mass can moderate the indoor peaks. Students used the single-node dynamic simulation familiar to them from the earlier experiments with passive-solar houses to estimate hourly variations in indoor temperature. Equation 7 shows the dynamic energy balance; the indoor temperature at the $n+1^{th}$ time step is a time-constant-weighted average of two terms from the previous time step, one due to heat gains and the other the indoor temperature. Heat gains are a sum of internal heat and resistance-weighted sol-air temperatures for the walls and windows, as defined in Equations 8 and 9.

$$T_{in,n+1} = R_{total}\, q_{eff}\left(1 - e^{-\frac{\Delta t}{\tau}}\right) + T_{in,n} e^{-\frac{\Delta t}{\tau}}$$

$$q_{eff} = q_{\mathrm{int},n} + \frac{T_{out,n}}{R_{airflow}} + \sum_i^{walls} \frac{T_{SAwall_i,n}}{R_{wall_i}} + \sum_j^{windows} \frac{T_{SAwindow_j,n}}{R_{window_j}} \tag{7}$$

$$T_{SA\,wall} = T_{out} + \frac{\alpha_{wall} \cdot I_t}{h_{out}} - \frac{\varepsilon_{wall} \cdot I_{LW}}{h_{out}} \tag{8}$$

$$T_{SA\,window} = T_{out} + \frac{SHGC \cdot I_t}{h_{out}} - \frac{\varepsilon_{window} \cdot I_{LW}}{h_{out}} \tag{9}$$

where R_{total} is the total thermal resistance, q_{int} is internal heat gain, T_{SA} is sol-air temperature, τ is the thermal time constant, α is absorptivity, I_t is total solar radiation, h_{out} is the outside-surface heat-transfer coefficient, ε is long-wave emissivity, SHGC is solar heat-gain coefficient and I_{LW} is net long-wave radiation. The long-wave-radiation terms in the sol-air-temperature equations apply only to horizontal surfaces.

A week-long warm-weather simulation, Figure 5, showed that with very high wind-driven airflows, 100 ACH, indoor temperatures will match outdoor temperatures. Internal heat is swept out and there is no tempering due to thermal mass. With lower airflows, 10 ACH, the mass dampens diurnal

temperature swings, as desired in warm weather; however, solar and internal gains will raise the mean temperature slightly above the mean outdoor temperature, as shown in Figure 6.

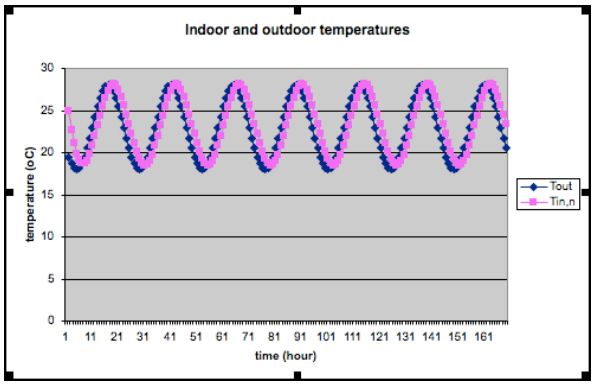

Figure 5. Outdoor and indoor temperatures for 100 ACH wind-driven natural ventilation.

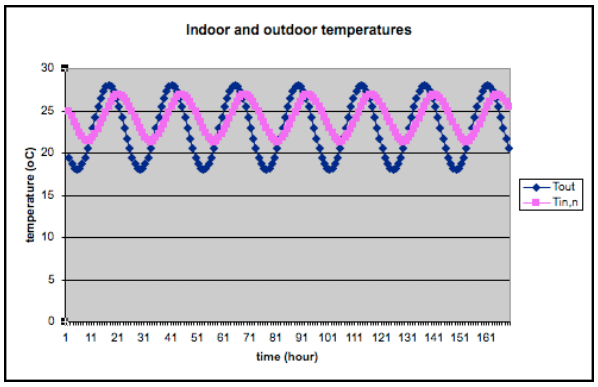

Figure 6. Outdoor and indoor temperatures for 10 ACH wind-driven natural ventilation.

EVAPORATIVE COOLING

Evaporative cooling was explored as a means of reducing indoor temperatures. As shown in a psychrometric chart, Figure 7, only September through November are appropriate. While it is well known that evaporative cooling follows a line of constant enthalpy on the psychrometric chart, the amount of cooling in passive processes in often unknown. Students tested three evaporative-cooling systems in the laboratory. In the first, strips of cotton, similar to what would be used in a shirt, were saturated with water and suspended in an air stream of about 2 m/s. The upstream relative humidity was 24%. The dry-bulb temperature dropped from 22.7 to 22.2 ^{o}C. In the second test, the air passed over open containers of water, dropping the temperature to 21.8 ^{o}C. In the third test, both previous methods were combined, dropping the air temperature to 20.7 ^{o}C, a sufficient drop to suggest that October temperatures could be reduced to the upper bound of the comfort region.

RAINFALL

Rainwater capture and potential use of photovoltaic panels were both assessed with straightforward bookkeeping and are briefly described here for completeness. Rainfall is highly seasonal, as displayed in Figure 2. Dry-season storage was considered essential by the designer, because the site does not include running water. The parking lot and the roofs of the three main buildings provide 457 m^2 of horizontal area potentially suitable for rain collection. Toilet flushes were estimated to be 242 per day and were considered to be the primary use of water. As shown in Table 3, 152 m^3 of excess rainwater can be stored in the rainy season in a tank of at least that size, leaving an annual deficit of 141 m^3. If only rainwater is to be used in the toilets, the number of flushes would need to be limited to 175 and the storage tank increased to at least 200 m^3. Finally, if the rainwater-collection area is increased to 634 m^2 and the storage tank to 293 m^3, there is adequate water for 242 flushes per day.

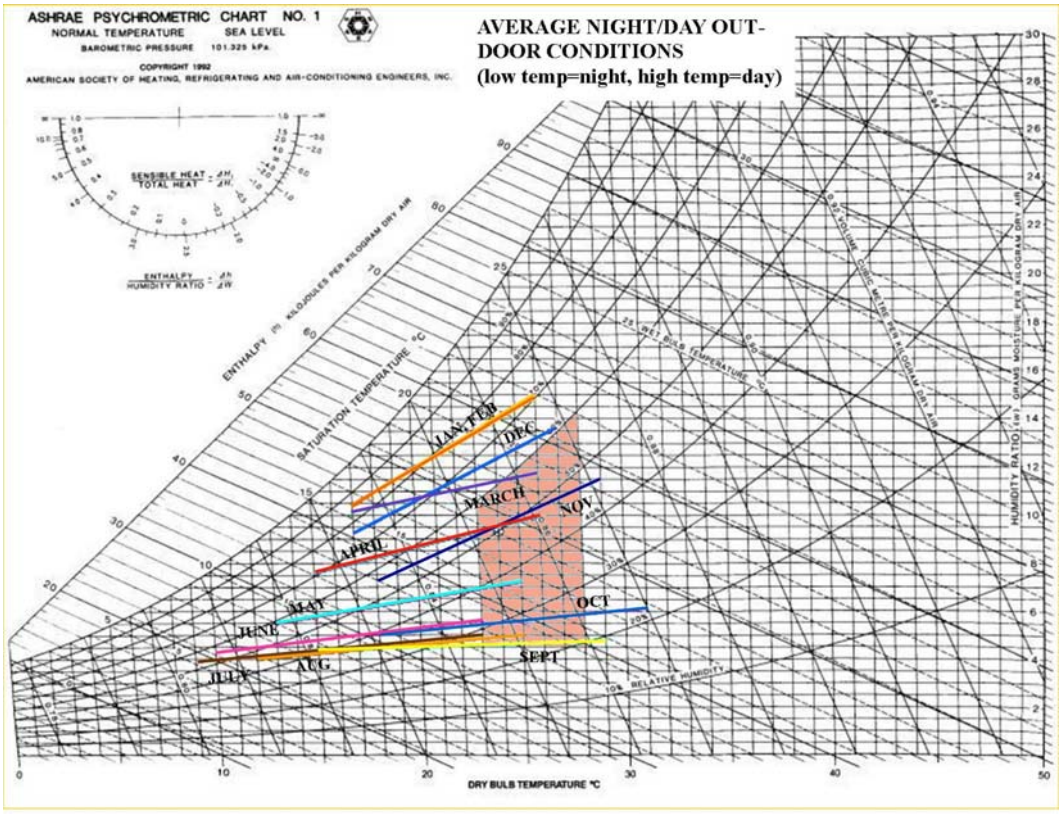

Figure 7. Psychrometric chart with monthly daytime and night dry-bulb temperatures and humidity ratios.

Table 3. Analysis of storage of rainwater.

month	Average rainfall, m^3	Rain collection area, m^2		
		457		634
		Water in excess of 242 flushes/day, m3	Water in excess of 175 flushes/day, m3	Water in excess of 242 flushes/day, m3
January	105.6	62.1	74.1	102.9
February	87.3	43.8	55.8	77.5
March	64.9	21.4	33.4	46.5
April	8.2	-35.3	-23.2	-32.1
May	1.4	-42.2	-30.1	-41.7
June	0	-43.6	-31.5	-43.6
July	0	-43.6	-31.5	-43.6
August	0	-43.6	-31.5	-43.6
September	0	-43.6	-31.5	-43.6
October	4.6	-39.0	-26.9	-37.2
November	41.6	-2.0	10.1	14.1
December	68.6	25.0	37.0	51.5
Water accumulated from rainy season		152.2	200.4	292.6
Annual excess from rainwater		-140.6	-5.8	7.2

PHOTOVOLTAIC PANELS

Lighting was considered by the designer to be the dominant electrical load. By dividing indoor space into low-light (100 lx) and high-light (750 lx) areas, students estimated that 94 15W compact fluorescent bulbs were adequate. For six-hour/day operation, monthly total electricity consumption was estimated to be 254 kWh. A PV system slightly less than 2 kW was designed to meet the load on a sunny day and would occupy 17 m^2 of roof area. The designer and client planned to ask for donated panels.

CONCLUSION

This project gave students an opportunity to thoughtfully combine measurements and simulations in support of a design of a necessarily low-energy building. Daylighting, ventilation and thermal balances were considered. The buildings were considered to be well-designed from the perspective of visual and thermal comfort. Questions were raised to the designer about the impact of interior walls; open trusses above the partition walls would promote ventilation for winds at oblique angles to the buildings, but would reduce acoustic privacy.

Physical airflow models were intuitive and easy to construct and locate relative to each other, and allowed students to work well as teams. More accurate results could have been obtained with skilled use of a CFD program but the course schedule would need to provide time for appropriate CFD instruction.

ACKNOWLEDGMENT

Prof. Jan Wampler provided the design of the buildings and site. Student work described in this paper was performed by Megan Arp, Christopher Barnes, Julia Bentcheva, Daniel Bergey, AnaLucia Berry, Gabriel Cira, Christopher Fematt, Qinyuan Liu, Maggie Nelson, Gavin Ruedisueli, Joseph Walsh, Shu Wang and Orlin Zhekov.

REFERENCES

ASHRAE. 2004. "ASHRAE Standard 55-2004. Thermal environmental conditions for human occupancy." ASHRAE, Atlanta.

BBC. 2006. "Average conditions, Lusaka, Zambia." http://www.bbc.co.uk/weather/world/city_guides/results.shtml?tt=TT000810

CONTAM. 2005. CONTAM Version 2.4. National Institute of Standards and Technology. http://www.bfrl.nist.gov/IAQanalysis/CONTAM/index.htm

Etheridge, D. and M. Sandberg. *Building ventilation: theory and measurement*. Wiley, Chicester.

IES. 2000. "The IESNA Lighting Handbook: Reference and Application." Illuminating Engineering Society of North America, New York.

Lightscape 1999. *Lightscape user's guide*. Autodesk. Lighting simulation is currently provided by Autodesk VIZ.

Mathworks. 2006. MATLAB 7.2. Natick, MA. www.mathworks.com

Walker, C. 2006. "Methodology for the evaluation of natural ventilation in buildings using a reduced-scale air model." Ph.D. thesis, Department of Architecture, Massachusetts Inst. of Technology, Cambridge, MA.

Washington Post. 2006. "Lusaka, Zambia historical weather data." http://www.washingtonpost.com/wp-srv/weather/longterm/historical/data/lusaka__zambia.htm.